J. Chem. Sci., Vol. 120, No. 6, November 2008, pp. 529–536.

Nanostructured phosphomolybdates†

J THOMAS[a], K R KANNAN[b] and A RAMANAN[a,*]

[a]Department of Chemistry, Indian Institute of Technology Delhi, New Delhi 110 016
[b]Solid State and Structural Unit, Indian Institute of Science, Bangalore 560 012
e-mail: aramanan@chemistry.iitd.ac.in

Abstract. Phosphomolybdate nanorods were synthesized using dodecyl pyridinium cations as structure directing agent. Composition and morphology of the nanorods were established by powder X-ray diffraction, energy dispersive X-ray analysis, fourier transform infrared spectroscopy, thermogravimetric analysis, transmission electron microscopy and scanning electron microscopy. Effect of synthetic variables such as pH and nature of templating agent on structure and morphology of the nanorods under ambient condition is discussed.

Keywords. Phosphomolybdates; nanorods; dodecyl pyridinium; electron microscopy.

1. Introduction

Aggregation of molecular units in solution (*bottom-up approach*) leads to solids (amorphous to crystalline) ranging from nano- to macro-dimensions.[1–3] However, understanding of supramolecular organization between soluble molecular species (chemically reasonable molecules)[4–6] leading to precipitation/crystallization of a particular solid is pertinent to appreciate self-assembly in terms of directing forces between reacting molecules during the phase separation. Moreover, synthetic parameters such as concentration of the reactants, pH of the reaction medium, organic template and temperature seem to influence the formation of a solid, its crystal structure as well as morphology including nanostructural features.[7,8] In this context, knowledge of structure-synthesis correlation is necessary so that reaction conditions can be systematically tuned to obtain specific crystal structure having desirable functionality, with control on the morphology, its distribution and dimension of precipitated/crystallized solids in terms of size (micro-to-nano).

For the past one decade, our group has been involved in the synthesis of porous and functionalized polyoxometalate based solids[9–11] to understand the role of organic templates and its influence on the self-assembly. Since these solids are potential catalytic materials for industrially important oxidation reactions,[12,13] tuning these into nano dimensions can provide an additional advantage for obtaining high turn over numbers. Recent research has shown that nanostructured vanadium and molybdenum oxides could be prepared by employing soft chemistry routes in the presence of long chain amines and surfactants.[14–17] Vanadium oxide nanotubes,[17] molybdenum oxide nanorods[18–20] are significant examples which show promising applications in the field of magnetism,[21] catalysis[22] and gas storage.[23] Recently, we have also demonstrated how phosphate incorporation can affect nanostructures of vanadium oxides.[24] In this paper, we present our results on how molybdenum oxide frameworks are modified upon substitution by phosphate units. Our earlier attempts to synthesize phosphomolybdate (PMO) based solids using organic amines viz. 1,2-diaminoethane,[25] 1,4-diaminobutane[26] and 1,4-diaminobenzene[27] under acidic aqueous conditions at room temperature resulted in $\{H_xP_2Mo_5O_{23}\}^{(6-x)-}$ cluster based solids (micron-sized crystals) while the presence of transition metal ions result in micron-sized multi-dimensional framework solids.[6] Here, we have investigated the growth of PMO solids in the presence of dodecyl pyridinium cations (DPC). Reacting molybdate and phosphate precursors with DPC under acidic conditions at room temperature resulted in nanorods (NRs) of high aspect ratio. Composition and morphology of the NRs were established by powder X-ray diffraction, energy dispersive X-ray analysis, fourier transform infrared spectroscopy, thermogravimetric analysis and electron microscopy. To the best of our knowledge, with reference to the

†Dedicated to Prof. C N R Rao on his 75th birthday
*For correspondence

PMO system there are no previous reports concerning nanostructures. Moreover, unlike vanadates, molybdates have rigid structural features and hence resulted in rod morphology.[17] The work is therefore significant in terms of understanding the self assembly of PMO solids.

2. Synthesis

All reagents were purchased from Aldrich and used as received. Sodium molybdate, $Na_2MoO_4{\cdot}2H_2O$ was used as molybdenum source and dodecyl pyridinium chloride as templating agent. Initially two different solutions were prepared. $Na_2MoO_4{\cdot}2H_2O$ (0·30 g, 1·25 mmol) was dissolved in 20 mL of water (solution A). Dodecyl pyridinium chloride (0·08 g, 0·31 mmol) was dissolved in 10 mL of water and the pH of the reaction medium was adjusted to ~1 using 1 M H_3PO_4 (solution B). Subsequently, solution A was added slowly to solution B with vigorous stirring. Immediately, white precipitate was obtained upon mixing of the two solutions. The resultant solution was stirred for 24 h and there after left undisturbed for two days. Finally, a yellow coloured precipitate was obtained which was washed with water and ethanol and dried in air. Scheme 1 shows the experimental procedure for synthesis.

3. Characterization

Fourier transform infrared (FTIR) spectra were recorded on KBr pellets using a Nicolet 5DX spectrophotometer. Thermogravimetric analysis (TGA) was done on Perkin-Elemer TGA7 from room temperature to 900°C at a heating rate of 10°C/min in nitrogen atmosphere to determine water and organic content

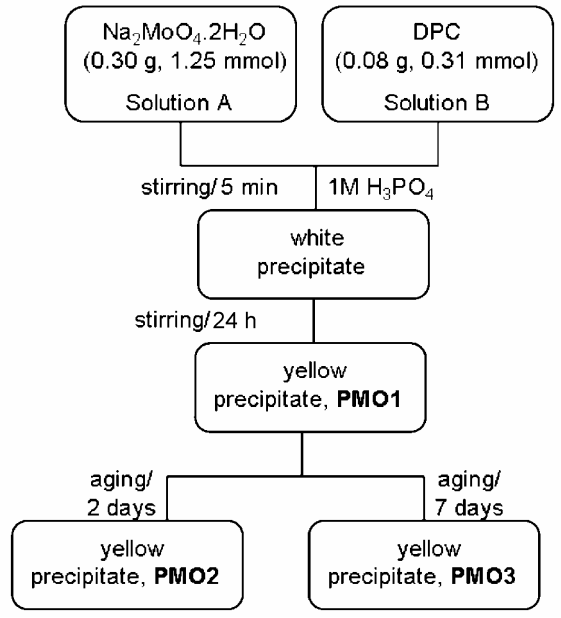

Scheme 1. Synthetic protocol for nanostructured PMOs.

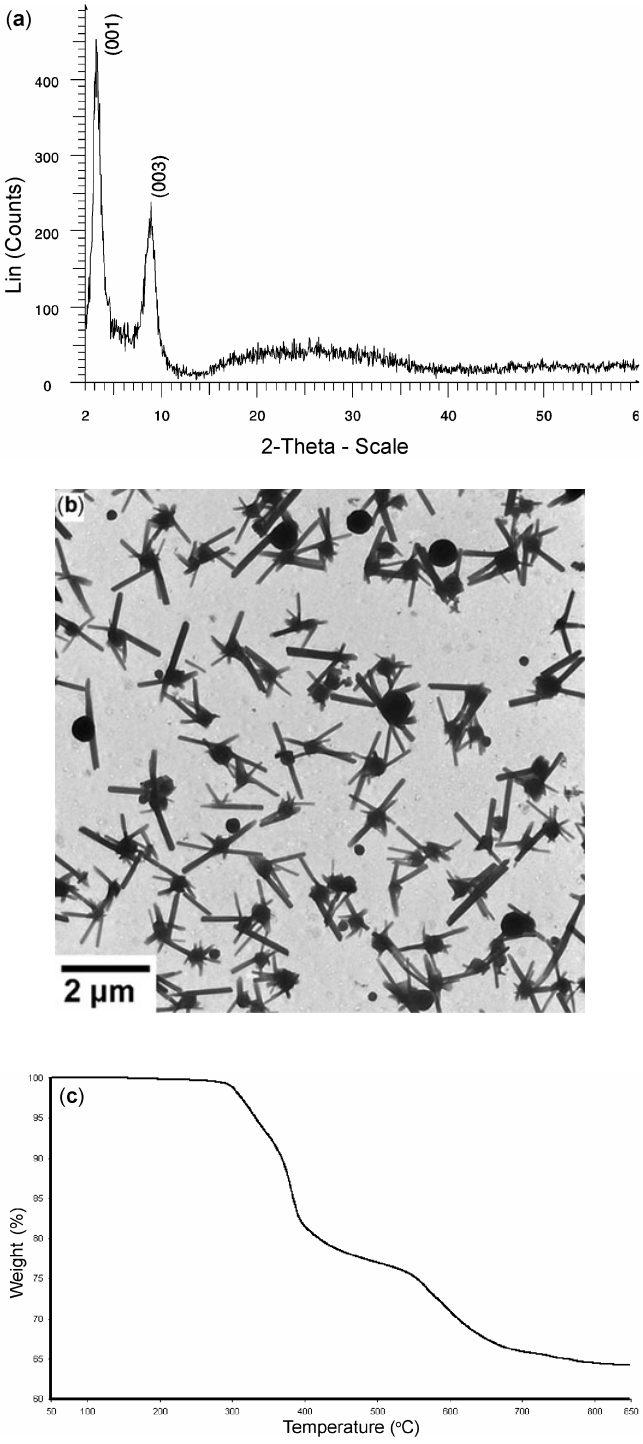

Figure 1. (**a**) PXRD, (**b**) TEM and (**c**) TGA of the product (**PMO2**) obtained at room temperature with molar ratio of DPC/$Na_2MoO_4{\cdot}2H_2O$ = 0·25 at pH ~1 upon 24 h of stirring followed by aging for two days.

as well as overall thermal stability of the product. Scanning electron microscopic studies (SEM) and energy dispersive X-ray analysis (EDAX) was carried out using JEOL5600LV and Oxford ISISI310 respectively. Powder X-ray diffraction data was collected on a Bruker D8 Advance diffractometer using Ni-filtered CuKα radiation. Data were collected with a step size of 0·02° and count time of 2*s* per step over the range $2° < 2\theta < 60°$. Transmission electron microscopic (TEM) studies were done on a Philips CM 20 electron microscope operated at 100 kV. Before TEM measurements the specimens were sonicated in absolute alcohol for 30 min and deposited on holey carbon-coated copper grids.

4. Results and discussion

The as-synthesized samples **(PMO2)** obtained were characterized by powder X-ray diffraction (PXRD). The presence of broad *00l* reflections in PXRD pattern (figure 1a) indicated lamellar characteristics having a *d*-spacing ~3·1 nm. Morphology and dimension of the product were characterized by TEM (figure 1b). It is apparent that the product contained rods of diameter ~70–100 nm and length up to 2 μm along with spherical particles of diameter ~300–700 nm. TGA (figure 1c) showed weight loss in the temperature region 200–380°C due to the decomposition of DPC moieties incorporated in the Mo-O-P framework. Total amount of DPC present in the sample was estimated to be ~45%. Loss of DPC occurred in two steps around 300 and 375°C. A third weight loss occurred at 545°C. After each weight loss the product obtained was characterized by FTIR and PXRD.

FTIR of the as-synthesized sample **(PMO2)** showed the presence of strong bands around 1063 and 962 cm^{-1} due to PO_4 groups, peaks around 962, 879, 800 and 679 cm^{-1} were attributed to Mo=O and Mo–O vibrations. Two absorption peaks at 2923 and 2852 cm^{-1} corresponded to the aliphatic C–H vibrations of DPC and a very broad peak centered at 3195 cm^{-1} was due to O–H stretching vibrations of the adsorbed water on the surface of the powders. Bands at the 1631 and 1488 cm^{-1} were attributed to extending vibrations of N–H and C–H respectively of DPC moiety.

After calcination at 300°C intensity of the peak corresponding to the O–H stretching vibrations weakened indicating desorption of water. However, the peaks at 2923, 2852, 1631 and 1488 cm^{-1} suggested that DPC was still retained in the solid. PXRD of the product after calcination showed peaks at *d*-spacing observed in **PMO2**. However, the intensity of diffraction peaks was diminished. This suggested that the composition and structure of the phase obtained was similar to **PMO2**. After calcination at 375°C the C–H vibration peaks disappeared suggesting the decomposition of DPC. PXRD pattern of the product was amorphous in nature. These observations suggested that ordered nanostructure cannot be preserved after thermal removal of the surfactant incorporated in the PMO framework. Finally, the PXRD of the product obtained after calcination at 545°C indicated the formation of crystalline

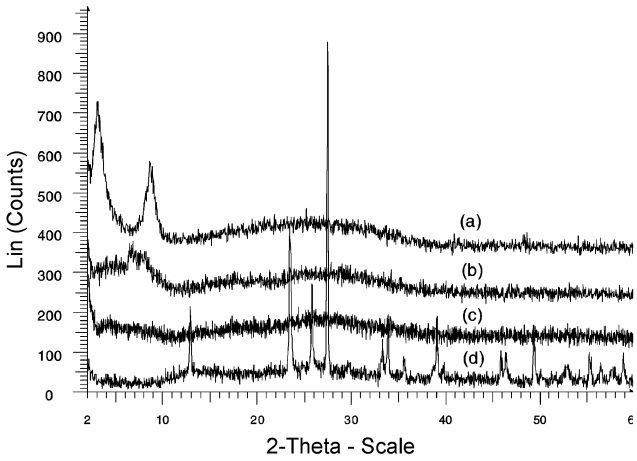

Figure 2. (**a**) PXRD of **PMO2**. PXRD of **PMO2** after heating for half an hour at (**b**) 300°C, (**c**) 375°C and (**d**) 545°C. All major peaks in (d) correspond to layered α-MoO_3.

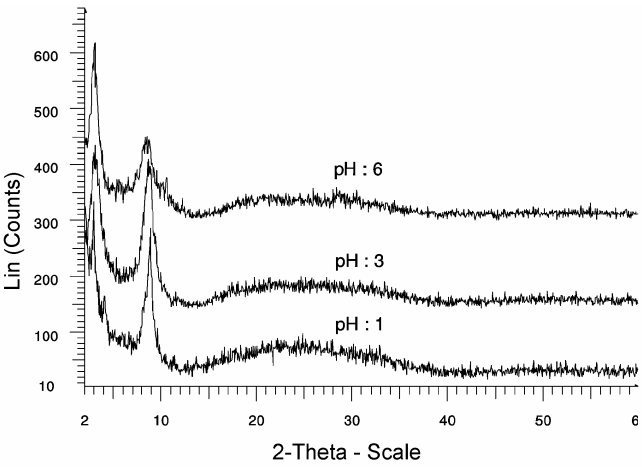

Figure 3. PXRD of the product obtained (**PMO2**) at room temperature with molar ratio of DPC/Na_2MoO_4·$2H_2O$ = 0·25 upon 24 h of stirring and aging for two days under acidic conditions.

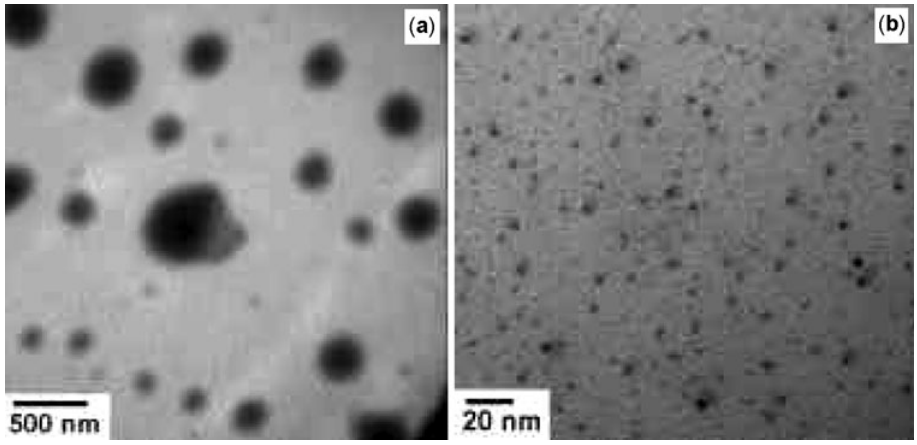

Figure 4. TEM of the product (**PMO2**) obtained at room temperature with molar ratio of DPC/$Na_2MoO_4{\cdot}2H_2O$ = 0·25 upon 24 h of stirring and aging for two days at (**a**) pH ~ 3 and (**b**) pH ~ 5.

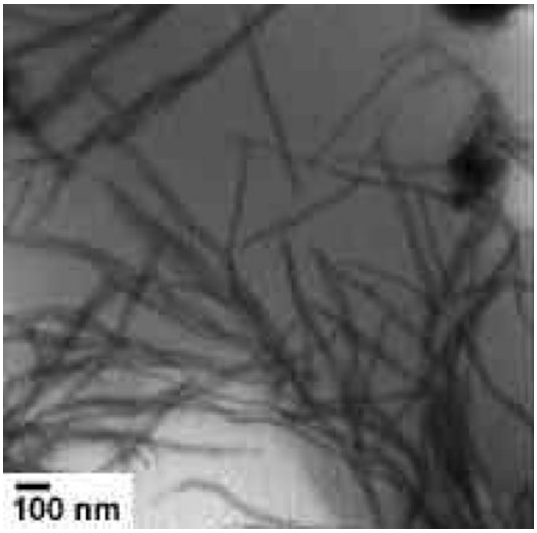

Figure 5. TEM of the product obtained at pH ~ 1 with molar ratio of CPC/$Na_2MoO_4{\cdot}2H_2O$ = 0·25.

α-MoO_3. Figure 2 shows the PXRD patterns of the products obtained after calcination. EDAX analysis indicated a molar ratio of P/Mo ~ 0·5. On the basis of TGA and EDAX, composition of NRs was found to be approximately as $(C_{17}H_{30}N)_3PMo_2O_{10}$.

4.1 *Influence of reaction parameters on the formation of nanorods*

Effect of reaction parameters such as pH of the reaction medium, nature of organic template and synthetic procedure on morphology of PMO nanostructures were studied. In what follows, effect of above parameters on the formation of nanostructured PMO is discussed.

4.1a *Influence of pH:* Effect of pH on formation of nanostructured PMO for molar ratio of DPC/$Na_2MoO_4{\cdot}2H_2O$ = 0·25 and stirring time of 24 h followed by two days of aging was investigated at room temperature. PXRD patterns suggested that the same phase was obtained under acidic pH (figure 3). However, TEM showed that morphology of the product varied with pH. At pH ~ 1, NRs of diameter ~ 70–100 nm and length ~ 0.2–1 μm along with particles of diameter ~ 300–700 nm were obtained. Increasing pH to ~ 3–5 resulted in the formation of particles but no well-defined NRs were seen. A further increase of pH into the basic range (pH > 7) yielded no precipitate. Figures 1b and 4 show TEM of the products obtained at pH 1, 3 and 5.

4.1b *Influence of template:* In addition to DPC, templating action of other cationic surfactants such as cetylpyridinium chloride (CPC) in the formation of PMO nanophases was explored. While in the case of DPC NRs were obtained, nanofibrils were obtained using CPC as shown in figure 5. The difference in the morphology could possibly be due to the increase in the carbon chain of the templating moiety.

4.1c *Synthesis under hydrothermal condition:* The effect of hydrothermal condition on the formation of nanostructures was explored using molar ratio of DPC/$Na_2MoO_4{\cdot}2H_2O$ = 0·25 and pH ~ 1. The reactants were heated in a teflon lined autoclave at 120°C for two days. Though PXRD of the product exhibited an intense peak at low angle (*d*-spacing ~ 3·0 nm), the features suggested multi-phasic nature of the product (figure 6a). An interesting observation to note was that precipitation at room tempera-

ture and hydrothermal condition affected the morphology of the nanostructures considerably. NRs with tapering ends of diameter ~ 80–200 nm and length up to 2 μm were observed (figure 6b). TGA showed weight loss in the temperature region 200–380°C due to the decomposition of DPC molecules incorporated in the Mo–O–P framework (figure 6c). Total amount of DPC present in the sample was estimated to be ~ 38%. EDAX analysis revealed P/Mo ratio around 0·5. On the basis of TGA and EDAX, overall composition of the product was estimated to be around $(C_{17}H_{30}N)PMo_2O_9$. Compositions of the nanophases obtained at room temperature and under hydrothermal conditions were almost similar except that the amount of organic incorporated was lower under hydrothermal condition.

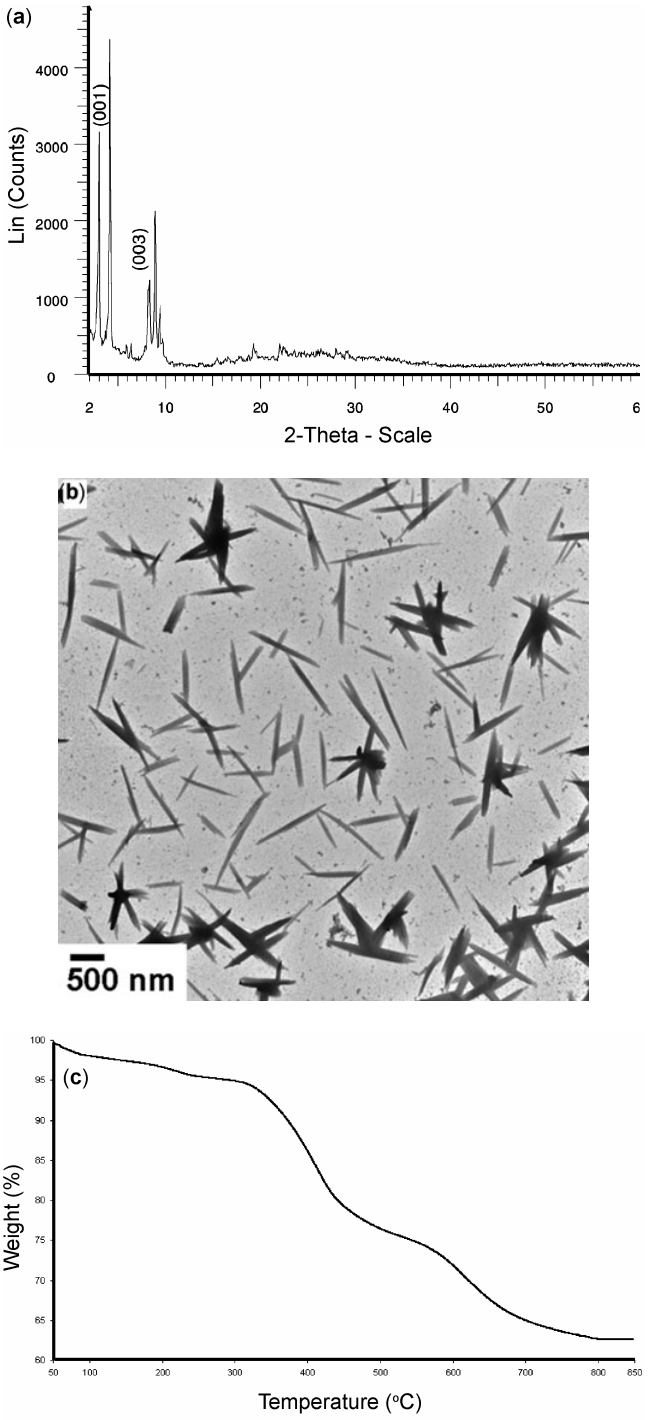

Figure 6. (**a**) PXRD, (**b**) TEM and (**c**) TGA of the product obtained under hydrothermal condition with molar ratio of DPC/$Na_2MoO_4{\cdot}2H_2O$ = 0·25 at pH ~ 1.

4.2 *Self-assembly of molybdates and organic amines*

Crystallization or precipitation of a solid is essentially a self assembly process. In aqueous solution, molybdate ions undergo continuous hydrolysis and condensation leading to a range of oligomeric anionic species; one or more of these self-assemble along with templates (organic amines as counter cations) or metal ions or both. Self-assembly is therefore dictated by supramolecular interactions between the reacting molecular units followed by condensation to form stable solids either cluster based or those which show extended interactions. During the past decade long chain amines and surfactants have been used extensively as templating agents.[16,17] It has been observed that if the solution contains considerable amount of reduced molybdate species, acidic conditions favour the formation of giant cluster based assemblies.[28,29] Incorporation of surfactant moieties under such condition leads to *surfactant encapsu-*

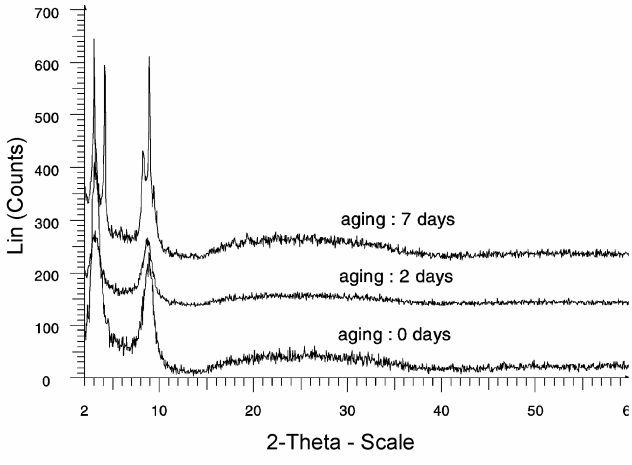

Figure 7. PXRD pattern of the products (**PMO1**, **PMO2** and **PMO3**) obtained at room temperature with molar ratio of DPC/$Na_2MoO_4{\cdot}2H_2O$ = 0·25 at pH ~ 1 upon 24 h of stirring and varying aging periods.

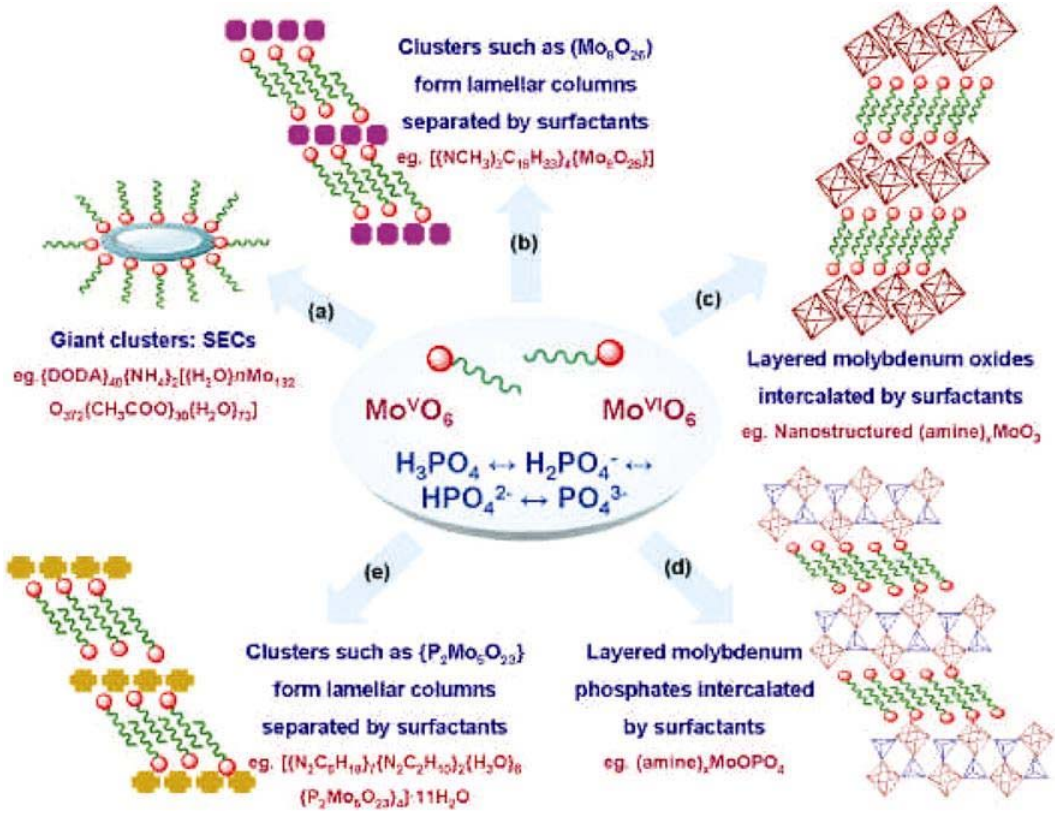

Scheme 2. Scheme shows the aggregation of long chain ammonium or surfactant cations around condensed molybdate and phosphomolybdate (PMO) species that are either oligomeric or extended. The green tail indicated hydrophobic part and red balls indicate hydrophilic polar part. (**a**) SECs observed in the case of giant molybdates.[31] (**b**) Cluster based surfactant aggregates.[32] (**c**) Surfactant intercalated nanostructured MoO_3.[15] (**d**) Layered phosphomolybdate solid intercalated with surfactant molecules.[33] (**e**) Phosphomolybdate cluster based solid incorporated with surfactant cations.[34] Nucleation of a surfactant incorporated solid is the result of a supramolecular organization directed by two major forces: (i) aggregation of ion-pairs of molybdate and/or phosphate anions and surfactant cations and (ii) ordering of surfactant cations through strong hydrophobicity.

lated clusters (SECs)[30,31] as shown in scheme 2. On the other hand, if the reaction medium contains only oxidized molybdate species, liquid crystal-like aggregation of surfactant molecules is observed; molybdenum oxide framework in the solid will thus be made of clusters, chains or sheets intercalated with surfactant cations.[15,16,19,32] Incorporation of phosphate units in the reaction medium will further modify the molybdenum oxide framework into various topologies. However, limited work has been reported in this regard. In the presence of organic amines oxidized molybdate species condense with phosphate units to form either layered or $\{P_2Mo_5O_{23}\}$ cluster based solids.[33,34] Aggregation of protonated surfactant moieties therefore occurs as columns between inorganic aggregates (refer scheme 2).

4.3 *Comments on growth mechanism of nanorods in the present study*

PMO species are negatively charged and therefore require electrostatic stabilization. This facilitates the formation of nanophases under acidic pH as it would favour the occurrence of DPC in protonated form. The formation of well defined nanophases under acidic conditions therefore seems obvious. To understand the growth of the nanophases under ambient conditions, $Na_2MoO_4{\cdot}2H_2O$ and DPC were taken in the molar ratio 0·25 at pH ~ 1 and stirred for 24 h and then allowed to age for different time intervals. The product obtained after aging were characterized by PXRD and TEM. The PXRD pattern of the products obtained without aging, **PMO1** and after 2 days of aging, **PMO2** showed broad *00l* reflections (figure 7)

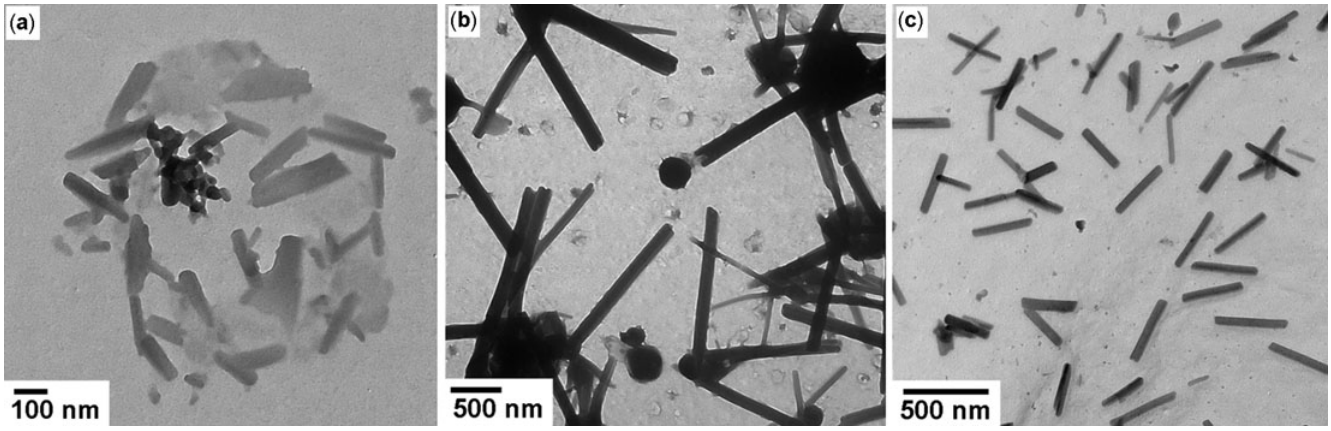

Figure 8. TEM of the product obtained at room temperature with molar ratio of DPC/$Na_2MoO_4 \cdot 2H_2O$ = 0·25 at pH ~ 1 upon 24 h of stirring and (**a**) without aging, **PMO1** (**b**) 2 days of aging, **PMO2** and (**c**) 7 days of aging, **PMO3**.

which indicates that probably liquid crystal-like aggregation of surfactant molecules is responsible for favouring lamellar characteristics. The PXRD pattern of the product aged for a week showed the formation of multi-phasic product (figure 7). It is most likely that an increase in the aging time favoured the growth of compositionally different phases. The corresponding TEM shown in figure 8 indicates a significant difference in the morphology of the products. While **PMO1** showed irregular morphology; NRs and particles were observed in the case of **PMO2**. After 7 days of aging NRs having diameter ~ 50–150 nm and length up to 2 μm were obtained. The absence of spherical particles upon aging suggests that coalesce of smaller particles leads to the formation of NRs.

5. Conclusions

In summary, formation of nanomaterials based on phosphomolybdates (PMOs) is reported for the first time. The results are significant considering the potential industrial interest in PMO-based solids. Like smaller organic templates, dodecylpyridinium ions also occur as counter cations but a favourable aggregation of surfactant ions (liquid-crystal like behaviour) restricts condensation of molybdate and phosphate units to lower-dimensions. However, rigidity of molybdate structural units favours the growth of PMO NRs rather than nanotubes unlike in the case of vanadates. Our process seems to offer a potentially low-temperature, low-cost and environmentally friendly way of producing single-phasic nano PMO.

Acknowledgements

JT thanks Honeywell International India Private Limited for research fellowship. AR thanks Department of Science and Technology (DST) for financial support as well as Powder X-ray Diffractometer under IRHPA to the Department of Chemistry, Indian Institute of Technology (IIT) Delhi, India. We acknowledge Department of Physics, IIT, Delhi for providing TEM facility.

References

1. Rao C N R 2001 *Curr. Sci.* **81** 1030
2. Rao C N R, Müller A and Cheetham A K (eds) 2004 *Chemistry of nanomaterials* (Weinheim: Wiley-VCH)
3. Jolivet J P 2000 *Metal oxide chemistry and synthesis: From solution to solid state* (Chichester: John Willey and Sons)
4. Ramanan A and Whittingham M S 2006 *Cryst. Growth Des.* **6** 2419
5. Thomas J and Ramanan A 2007 *Curr. Sci.* **93** 1664
6. Thomas J and Ramanan A 2008 *Cryst. Growth Des.* **8** 3390
7. Mann S 2000 *Angew. Chem. Int. Ed.* **39** 3392
8. Long D-L, Burkholder E and Cronin L 2007 *Chem. Soc. Rev.* **36** 105
9. Pope M T and Müller A 1994 In *Polyoxometalates: From platonic solids to anti-retroviral activity* (Dordrect: Kluwer)
10. Yamase T and Pope M T 2002 *Polyoxometalate chemistry for nano-composite design* (Berlin: Springer)
11. Ishii Y, Takenaka Y, Konishi, K and Presto 2004 *Angew. Chem.* **116** 2756
12. Hill C L 1996 *Polyoxometalates in catalysis,* Elsevier

13. Kozhevnikov I 2002 *Catalysis by polyoxometalates: Catalysis by polyoxometalates Vol. 2* (Chichester: John Willey and Sons)
14. Spahr M E, Bitterli P, Nesper R, Müller M, Krumeich F and Nissen H U 1998 *Angew. Chem. Int. Ed.* **37** 1263
15. Niederberger M, Krumeich F, Muhr H J, Müller M and Nesper R 2001 *J. Mater. Chem*. **11** 1941
16. Patzke G R, Krumeich F and Nesper R 2002 *Angew. Chem. Int. Ed*. **41** 2446
17. Thomas J, Asnani M, Sharma S and Ramanan A 2008 *Nanostructure vanadium oxides* in *encyclopedia of nanoscience and nanotechnology* (USA: American Scientific Publishers)
18. Satishkumar B C, Govindaraj A, Nath M and Rao C N R 2000 *J. Mater. Chem.* **10** 2115
19. Patzke G R, Michailovski A, Krumeich F, Nesper R, Grunwaldt and Baiker A 2004 *Chem. Mater.* **16** 1126
20. Michailovski A and Patzke G R 2006 *Chem. Eur. J.* **12** 9122
21. Krusin-Elbaum L, Newns D M, Zeng H, Derycke V, Sun J Z and Sandstrom R 2004 *Nature* **431** 672
22. Chen X W, Zhu Z, Havecker M, Su D S and Schlögl R 2007 *Mater. Res. Bull.* **42** 354
23. Taurino A M, Forleo A, Francioso L, Siciliano P, Stalder M and Nesper R 2006 *Appl. Phys. Lett.* **88** 152111
24. Asnani M, Thomas J and Ramanan A 2007 *Mater. Res. Bull.* **42** 686
25. Asnani M 2006 *Framework solids, mesophases and nanostructures of organically templated vanadium and molybdenum phosphates* Ph D thesis, Indian Institute of Technology Delhi, India
26. Upreti S and Ramanan A 2005 *Acta Crystallogr.* **E61** m414
27. Upreti S and Ramanan A 2006 *Cryst. Growth Des.* **6** 2066
28. Müller A and Serain C 2000 *Acc. Chem. Res.* **33** 2
29. Müller A and Roy S 2003 *Coord. Chem. Rev.* **245** 153
30. Kurth D G, Lehmann P, Volkmer D, Cölfen H, Koop M J, Müller A and Chesne A D 2000 *Chem. Eur. J.* **6** 385
31. Kurth D G, Lehmann P, Volkmer D, Müller A and Schwahn D 2000 *J. Chem. Soc., Dalton Trans.* 3989
32. Spahr M E and Nesper R 2001 *Z. Anorg. Allg. Chem.* **627** 2133
33. Rangan K K and Gopalakrishnan J 1996 *Inorg. Chem.* **35** 6080
34. Liu Z, Wang E, Wang L, Xu L, Xing Y, Lin Y and Jia H 1999 *Fenzi Kexue Xuebao* **15** 140